



Delft University of Technology

## Indoline Catalyzed Acylhydrazone/Oxime Condensation under Neutral Aqueous Conditions

Zhou, Yuntao; Piergentili, Irene; Hong, Jennifer; van der Helm, Michelle P.; Macchione, Mariano; Li, Yao; Eelkema, Rienk; Luo, Sanzhong

### DOI

[10.1021/acs.orglett.0c02128](https://doi.org/10.1021/acs.orglett.0c02128)

### Publication date

2020

### Document Version

Final published version

### Published in

Organic Letters

### Citation (APA)

Zhou, Y., Piergentili, I., Hong, J., van der Helm, M. P., Macchione, M., Li, Y., Eelkema, R., & Luo, S. (2020). Indoline Catalyzed Acylhydrazone/Oxime Condensation under Neutral Aqueous Conditions. *Organic Letters*, 22(15), 6035-6040. <https://doi.org/10.1021/acs.orglett.0c02128>

### Important note

To cite this publication, please use the final published version (if applicable).  
Please check the document version above.

### Copyright

Other than for strictly personal use, it is not permitted to download, forward or distribute the text or part of it, without the consent of the author(s) and/or copyright holder(s), unless the work is under an open content license such as Creative Commons.

### Takedown policy

Please contact us and provide details if you believe this document breaches copyrights.  
We will remove access to the work immediately and investigate your claim.

# Indoline Catalyzed Acylhydrazone/Oxime Condensation under Neutral Aqueous Conditions

Yuntao Zhou, Irene Piergentili, Jennifer Hong, Michelle P. van der Helm, Mariano Macchione, Yao Li, Rienk Eelkema,\* and Sanzhong Luo\*



Cite This: *Org. Lett.* 2020, 22, 6035–6040



Read Online

ACCESS |



Metrics & More

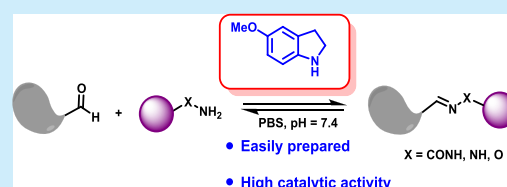


Article Recommendations



Supporting Information

**ABSTRACT:** Acylhydrazones formation has been widely applied in materials science and biolabeling. However, their sluggish condensation rate under neutral conditions limits its application. Herein, indolines with electron-donating groups are reported as a new catalyst scaffold, which can catalyze acylhydrazone, hydrazone, and oxime formation via an iminium ion intermediate. This new type of catalyst showed up to 15-fold rate enhancement over the traditional aniline-catalyzed reaction at neutral conditions. The identified indoline catalyst was successfully applied in hydrogel formation.



The acylhydrazone/hydrazone and oxime formation<sup>1</sup> are fundamental condensation reactions, widely utilized in different fields including dynamic combinatorial chemistry,<sup>2</sup> bioconjugation,<sup>3</sup> polymer chemistry,<sup>4</sup> stimuli responsive materials, and soft materials.<sup>5</sup> However, the slow rate of these condensations under neutral aqueous conditions has limited their applications in biological contexts. Therefore, there have been tremendous efforts to improve the reaction rate.<sup>6</sup> In 1960s, Jencks reported aniline as a nucleophilic catalyst for hydrazone (semicarbazone) formation via transamination of an imine intermediate.<sup>7</sup> Later on, this catalysis was shown to work well under biological conditions (Figure 1).<sup>3,8</sup> A number of aniline derivatives with improved catalytic

effective catalyst, 5-methyl-2-aminobenzenephosphonic acid.<sup>10</sup> Recently, Roelfes and co-workers reported an artificial enzyme featuring *p*-aminophenylalanine anchoring into the hydrophobic pocket as a catalytic residue.<sup>11</sup> Compared with aniline, the designed aniline-enzyme showed a more than 2 orders of magnitude rate increase for hydrazone and oxime formation.

Despite these prominent advances, most of these catalysts rely on the primary aniline motif. The secondary amines, which have been widely employed in asymmetric organocatalysis,<sup>12</sup> were generally overlooked for catalysis of acylhydrazone/hydrazone and oxime formation, although aliphatic secondary amines have been included for screening, showing only poor activity.<sup>9b</sup> We hypothesized that secondary aromatic amine would serve as an effective catalyst for acylhydrazone/hydrazone and oxime formation at neutral pH (Figure 1). Compared with primary aniline, secondary aromatic amines would condense to form an iminium ion intermediate; enhanced electrophilicity relative to the typical imine intermediate with aniline (Figure 1) is anticipated due to its positively charged nature particularly under neutral pH conditions. Herein, we report that easily prepared indoline derivatives with electron-donating groups effectively accelerate acylhydrazone/hydrazone and oxime formation, enhancing the reaction rate considerably compared to the traditional aniline-catalyzed reaction at neutral pH. The new catalysts are active on a wide substrate scope. 5-Methylindoline successfully enhanced the rate of supramolecular gel formation at neutral

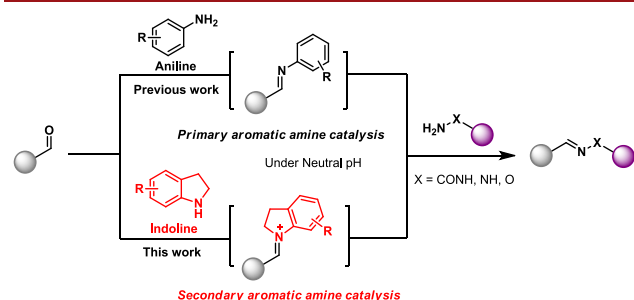


**Figure 1.** Acylhydrazone/hydrazone and oxime formation via indoline catalysis.

ability have been developed. For example, Kool developed bifunctional anilines with acid/base groups ortho to the amino group such as 5-methoxyanthranilic acid, 2-aminophenols, and 2-(aminomethyl)benzimidazoles.<sup>9</sup> The bifunctional catalysis was ascribed to the enhanced formation of the imine intermediate via intramolecular H-bonding, and an up to 7-fold rate increase over aniline was observed with the most

**Received:** June 27, 2020

**Published:** July 29, 2020



pH, including a particularly challenging formation of potentially antiviral gel materials.

To obtain more effective catalysts, we investigated the condensation between 4-nitrobenzaldehyde and benzoylhydrazine as a model reaction (Scheme 1). All reactions were

Scheme 1. Screening of Catalysts<sup>a</sup>

Entry	catalyst	$k_{app}(M^{-1}s^{-1})$	$k_{rel}$	Entry	catalyst	$k_{app}(M^{-1}s^{-1})$	$k_{rel}$
1		0.030 ± 0.002	1.00	10		0.151 ± 0.003	5.03
2		0.110 ± 0.005	3.66	11		0.057 ± 0.001	1.90
3		0.093 ± 0.002	3.10	12		0.019 ± 0.001	0.63
4		0.214 ± 0.006	7.13	13		0.178 ± 0.003	5.93
5		0.116 ± 0.001	3.86	14		0.465 ± 0.024	15.50
6		0.065 ± 0.007	2.16	15		0.329 ± 0.023	10.96
7		0.075 ± 0.003	2.50	16		0.227 ± 0.014	7.56
8		0.026 ± 0.007	0.86	17		0.063 ± 0.005	2.10
9		0.573 ± 0.082	19.10	18		0.037 ± 0.001	1.23

<sup>a</sup>Apparent second-order rate constants,  $k_{app}$  ( $M^{-1} s^{-1}$ ), are given as mean values  $\pm$  standard deviations based on triplicate measurements or more. Conditions: 123 mM NaCl, 2.4 mM KCl, and 10.7 mM sodium and potassium phosphate (pH 7.4) with 10% DMF as cosolvent.

performed under pseudo-first-order conditions in phosphate buffered saline (PBS) at pH 7.4 with 10% DMF as cosolvent. Apparent second-order rate constant  $k_{app}$  ( $M^{-1} s^{-1}$ ) values were obtained by monitoring UV–vis absorption at 329 nm of the hydrazone product. To calculate the rate constants we used nonlinear regression by linear least-squares fits, following the Guggenheim method (for details, see Supporting Information).<sup>6b,13</sup> The observed rate increases linearly for both 4-nitrobenzaldehyde and catalyst under excess concentration, indicating the reaction is first order for each substrates and catalyst (see Supporting Information, Figure S1d). Generally, acylhydrazone formation is more challenging than hydrazone formation under neutral aqueous conditions. Without catalysis, the model reaction is too slow to reach equilibrium in pH = 7.4 within 24 h.

Selected screening results are shown in Scheme 1. Aniline ( $pK_a = 4.6$  in  $H_2O$ )<sup>3a,7a</sup> was selected as the reference (entry 1). A range of primary amine catalysts including the well-explored aniline analogue catalysts were also investigated for comparison.<sup>9,10</sup> Among all the primary amine catalysts examined (Scheme 1, entries 1–9), 5-methyl-2-aminobenzophosphonic acid, previously reported by Kool,<sup>10a</sup> showed good catalytic effects, with a  $0.573 M^{-1} s^{-1}$  apparent rate constant

and 19.10 times rate enhancement over aniline (Scheme 1, entry 9 vs entry 1). We first tested our secondary amine hypothesis with *N*-methylaniline. Unfortunately, *N*-methylaniline and its derivatives bearing either *para*-methoxy or *ortho*-carboxylic acid displayed negligible catalytic effects. Other cyclic aromatic secondary amines were examined. To our delight, we found that indoline ( $pK_a = 5.6$ )<sup>14</sup> showed moderate catalytic activity for the model reaction, with a 5.0-fold rate enhancement (entry 10) over that of aniline. In contrast, 1,2,3,4-tetrahydro-quinoline ( $pK_a = 4.7$ )<sup>14</sup> showed poor catalytic activity (not shown). Pyrrolidine ( $pK_a = 11.2$ ) was also inactive under the present conditions, which may suggest that the benzene ring decreases the basicity of nitrogen in indoline and stabilizes the iminium intermediate under aqueous solution, which pinpoints the importance of aromatic amino-catalysis.<sup>15</sup> All these results confirm the concept that the  $pK_a$  of catalysts closest to the neutral buffer solution provide more rate enhancements for acylhydrazone/hydrazone formation.<sup>3a,10a,16</sup>

Finding the indoline scaffold prompted us to improve its activity, and indolines with different substitutions were investigated next. Most substituted indolines are commercially available or easy to prepare in high yields (for details, see Supporting Information).<sup>17</sup> Inspired by Kool's work,<sup>9,10</sup> indoline derivatives with carboxylic acid groups in the 2- and 7-positions were first explored. Unexpectedly, indoline-2-carboxylic acid (entry 11) shows the  $k_{app}$  was  $0.057 M^{-1} s^{-1}$ , only 1.90 times faster than aniline, while indoline-7-carboxylic acid was virtually inactive. Compared with indoline, 2-methylindoline (entry 12) showed a substantial reduction in catalytic efficiency, likely a result of a steric effect on iminium formation. However, 7-hydroxyindoline (entry 13) showed slightly higher activity. 7-aza-Indoline endowed with a fused pyridinyl ring had no catalytic activity at all.

Next the substitution effects on the benzene ring of indoline were examined (entries 14–18). Indolines with electron-donating groups showed enhanced reaction rates. For example, 5-methylindoline (entry 15) showed a 11-fold rate enhancement, and 5-methoxyindoline (entry 14) showed enhancement up to 15.50-fold, comparable to 5-methyl-2-aminobenzophosphonic acid (entry 9). With increasing electron-withdrawing ability, the reaction rate dramatically decreased (entries 16–18) and 5-nitroindoline (not shown) showed no activity. A good linear relationship was obtained when the logarithm of rate constants  $\log k_x/k_H$  was plotted against Hammett substitute constant  $\sigma$  (Figure 2, black line). A large negative slope ( $\rho = -1.804$ ) reveals the electron-deficient nature of the key reaction species in the rate-limiting step,

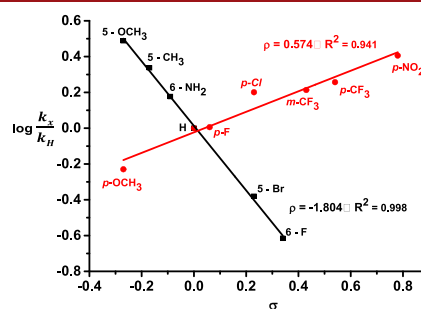
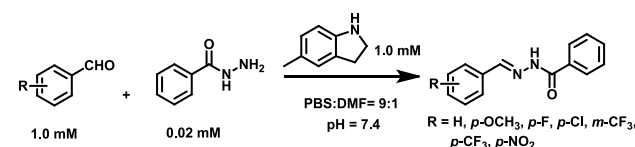


Figure 2. Hammett plot of substitution effects of indoline (black) and benzaldehydes (red).

characteristic of an iminium ion species in the current catalysis. We also explored the electronic effect on benzaldehydes (Scheme 2). The catalysis seems to be less dependent on the

Scheme 2. Substitution Effects of Benzaldehyde



electronic nature of the substrates (Figure 2, red line), but slightly favors electron-deficient benzaldehydes, consistent with their enhanced iminium ion formation and reactivity.

Moreover, the pH effect of the current indoline catalysis was also examined by increasing the solution pH in phosphate buffered saline for acylhydrazone formation (see Supporting Information, Figure S7 and Table S1). Across the pH range from 4.5 to 7.4, the indoline catalysis was faster than that of aniline. The acidic condition could enhance the rate of aniline catalysis; even under this condition (e.g., pH = 5.0), the catalysis with indoline was still substantially faster (Table S1). This observation highlights the beneficial secondary amine motif that is feasible for iminium ion catalysis regardless of pH.

With the optimized catalyst in hand, we next examined its scope (Scheme 3 and 4). Aliphatic acylhydrazides including

Scheme 3. Scope of Nucleophiles<sup>a</sup>

Reaction scheme showing the catalytic reaction of 4-nitrobenzaldehyde (1.0 mM) with various nucleophiles (R-X-NH<sub>2</sub>, 0.02 mM) in PBS:DMF = 9:1 at pH 7.4, catalyzed by indoline (1.0 mM).

Entry	R-X-NH <sub>2</sub>	Aniline	Indoline	5-Methoxyindoline	5-Methoxyindoline-PO <sub>3</sub> H <sub>2</sub>
1	Aliphatic acylhydrazide	0.030±0.002	0.147±0.003	0.316±0.026	0.697±0.035
2	Aliphatic acylhydrazide	0.035±0.001	0.162±0.003	0.365±0.004	0.650±0.001
3	Salicylaldehyde	0.268±0.009	1.634±0.091	2.823±0.127	1.743±0.085
4	Picolinaldehyde	0.058±0.005	0.245±0.005	0.784±0.038	0.241±0.004
5	Phenylhydrazide	0.137±0.005	0.639±0.010	2.770±0.221	1.997±0.110
6	Phenylhydrazide	0.413±0.007	0.493±0.017	2.440±0.340	9.910±0.036

<sup>a</sup>Apparent second-order rate constant  $k_{app}$  (M<sup>-1</sup> s<sup>-1</sup>) was measured under the same conditions as listed in Scheme 1).

bulky ones were compatible with indoline catalysis. Indoline was 5-fold faster than aniline (Scheme 3, entries 1 and 2), and the optimal 5-methoxyindoline was 10 times faster. In these cases, indoline catalysis is comparable but slightly slower than the best reported aniline phosphonic acid catalyst. The catalysis also worked well with functionalized arene acylhydrazides such as salicylhydrazide or picolinylhydrazide, and up to 13-fold-rate enhancement over aniline could be achieved (Scheme 3, entries 3 and 4). In these cases, indoline catalysts performed much better than the aniline phosphonic acid

Scheme 4. Scope of Aldehydes<sup>a</sup>

Reaction scheme showing the catalytic reaction of various aldehydes (R-CHO, 1.0 mM) with benzoylhydrazine (0.02 mM) in PBS:DMF = 9:1 at pH 7.4, catalyzed by indoline (1.0 mM).

Entry	R-CHO	Aniline	Indoline	5-Methoxyindoline	5-Methoxyindoline-PO <sub>3</sub> H <sub>2</sub>
1	4-Methoxybenzaldehyde	0.014±0.009	0.049±0.005	0.092±0.007	0.259±0.013
2	2-Thienaldehyde	0.007±0.002	0.035±0.001	0.086±0.008	0.065±0.002
3	Picolinaldehyde	0.135±0.004	0.776±0.005	2.195±0.065	2.304±0.036
4	Salicylaldehyde	0.082±0.006	0.150±0.003	0.364±0.024	0.816±0.023
5	Quinoline-8-carbaldehyde	1.048±0.057	1.689±0.097	4.953±0.188	10.880±0.267
6	Glyoxylic acid	0.789±0.062	4.340±0.053	14.510±0.518	4.445±0.021

<sup>a</sup>Apparent second-order rate constant  $k_{app}$  (M<sup>-1</sup> s<sup>-1</sup>) was measured under the same conditions as listed in Scheme 1.

catalyst, highlighting its applicability and functional group tolerance. Indoline catalysis was also found to promote hydrazone and oxime formation effectively (Scheme 3, entries 5 and 6). In oxime formation, the indoline catalysis is 20 times faster than aniline, representing the most efficient catalysis examined.<sup>18</sup>

The scope of aldehyde substrates was explored with benzoylhydrazine as a model (Scheme 4). Electron-rich aldehydes such as 4-methoxyaldehyde and 2-thienaldehyde are sluggish substrates, and the application of 5-methoxyindoline catalysis led to 6-fold and 12-fold enhancement, respectively (Scheme 4, entries 1 and 2). Aromatic aldehydes such as picolinaldehyde, quinoline-8-carbaldehyde, and salicylaldehyde were also used and 5-methoxyindoline and 5-methyl-2-aminobenzene phosphonic acid demonstrated comparable performance (Scheme 4, entries 3–5). Interestingly, glyoxylic acid showed the highest rates (14.51 M<sup>-1</sup> s<sup>-1</sup>, Scheme 4, entry 6) among all the examined substrates with indoline catalysis. Aliphatic aldehyde and unactivated ketones have also been examined; unfortunately indoline did not show effective catalysis in these cases.

Having discovered substituted indolines as efficient catalysts for hydrazone formation under neutral conditions, we then turned our attention to its application in biomedical materials. In the past, we reported how the formation and the mechanical properties of low molecular weight (LMW) hydrazone hydrogelators can be controlled directly by catalytic action (Figure 3a).<sup>5a</sup> In those systems, control over the rate of hydrazone formation is crucial to achieve local gel formation, control gel object dimensions, and properties.<sup>19</sup>

The rate of hydrazone formation was mostly controlled using acid catalysis. When using aniline at neutral pH, the electron-rich benzaldehyde substrates gave sluggish reactions, limiting application at neutral pH. Recently, we became interested in applying these hydrogels as broad spectrum antiviral materials, inspired by the work of Stellacci, Lembo,



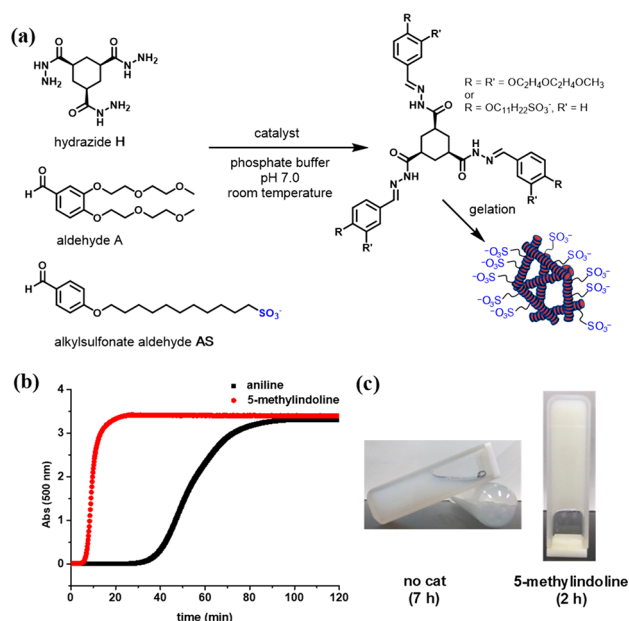


**Figure 3.** (a) Catalyzed trishydrazide hydrogelator formation. (b) The turbidity measurements at 500 nm. (c) Inverted vial method tests of hydrogelator formation and appearance with or without 5-methylindoline. For (b) and (c), samples were prepared by mixing stock solutions of 8 mM acylhydrazide H, 48 mM aldehyde A, with or without 10 mM catalyst (aniline or 5-methylindoline) in 0.1 M phosphate buffer at pH 7.0.

and Jones.<sup>20</sup> For this purpose, it is crucial that we can generate gel fibers that have a high density of alkylsulfonate groups, preferably at neutral pH. These decorated fibers can be made by reaction and subsequent *in situ* gelation of a mixture of trishydrazide H, benzaldehyde A, and alkylsulfonate benzaldehyde AS (Figure 3).<sup>21</sup> To investigate the potential of indoline catalysis, we first looked at gel formation without the sulfonate. In the reaction between H and A, turbidity measurements were used to monitor the rate of hydrogel fiber formation. 5-Methylindoline and aniline were selected as catalysts. All experiments were performed in 0.1 M phosphate buffer at pH 7.0. As shown in Figure 3b, the turbidity developed much earlier and at a higher rate when using 5-methylindoline than when using aniline (for details, see Supporting Information, Figure S8). The gelation time, as determined by the inverted vial method, was within 2 h for the 5-methylindoline catalyzed sample while the uncatalyzed sample remained a liquid suspension even after 7 h ([H] = 8 mM, Figure 3c). Rheological measurements showed that 5-methylindoline catalyzed gelation gives a constant  $G'$  of 6 kPa, 50 min after starting the reaction. Aniline catalysis leads to  $G' = 5$  kPa after 110 min, confirming the trends observed in the turbidity measurements and in the small molecule models (for details, see Supporting Information, Figure S9). Moreover, when [H] = 20 mM was used, the uncatalyzed reaction required 8 h to gel. Using 10 mM aniline, this time is reduced to 3 h, whereas 10 mM 5-methyl indoline further reduces it, providing a gel within 2 h (for details, see Supporting Information, Table S2).

Next, we used a mixture of A and AS aldehydes (30 mol % sulfonated aldehyde AS) in the gelation. In the absence of catalyst, these mixtures require over 6 h to form a gel ([H] = 20 mM). When we used 5-methyl indoline as a catalyst (10 mM), these mixtures gelled in 1.5 h, forming stable and stiff

gels with a slight yellow color on account of oxidized indoline (see Supporting Information, Figure S10).

In summary, we have shown that easily prepared indoline derivatives bearing a secondary amine in the catalytic center can act as new efficient catalysts for acylhydrazide/oxime formation under neutral aqueous conditions. The reaction rates are faster than the typical primary amine aniline-catalyzed reactions at neutral pH. Indoline is comparable with the most effective catalyst reported to date, 5-methyl-2-aminobenzene phosphonic acid, and shows better reactivity for some substrates. The benzene ring is crucial for indoline catalysis, and electron-donating groups increase the catalytic activity by stabilizing the formation of highly active iminium intermediates. The new catalysts were investigated for a broad substrate scope and were successfully used to accelerate hydrogel formation for challenging biomedical substrates under neutral pH conditions.

## ■ ASSOCIATED CONTENT

### Supporting Information

The Supporting Information is available free of charge at <https://pubs.acs.org/doi/10.1021/acs.orglett.0c02128>.

Synthesis of indoline derivatives, experimental details, kinetic fit data analysis, absorbance spectra, pH effect, NMR spectra, gel formation and rheology test, and supporting figures (PDF)

## ■ AUTHOR INFORMATION

### Corresponding Authors

**Sanzhong Luo** – Center of Basic Molecular Science (CBMS), Department of Chemistry, Tsinghua University, Beijing 100084, China; [orcid.org/0000-0001-8714-4047](https://orcid.org/0000-0001-8714-4047); Email: [luosz@tsinghua.edu.cn](mailto:luosz@tsinghua.edu.cn)

**Rienk Eelkema** – Department of Chemical Engineering, Delft University of Technology, 2629HZ Delft, The Netherlands; [orcid.org/0000-0002-2626-6371](https://orcid.org/0000-0002-2626-6371); Email: [R.Eelkema@tudelft.nl](mailto:R.Eelkema@tudelft.nl)

### Authors

**Yuntao Zhou** – Center of Basic Molecular Science (CBMS), Department of Chemistry, Tsinghua University, Beijing 100084, China

**Irene Piergentili** – Department of Chemical Engineering, Delft University of Technology, 2629HZ Delft, The Netherlands; [orcid.org/0000-0002-2220-4157](https://orcid.org/0000-0002-2220-4157)

**Jennifer Hong** – Department of Chemical Engineering, Delft University of Technology, 2629HZ Delft, The Netherlands

**Michelle P. van der Helm** – Department of Chemical Engineering, Delft University of Technology, 2629HZ Delft, The Netherlands

**Mariano Macchione** – Department of Chemical Engineering, Delft University of Technology, 2629HZ Delft, The Netherlands

**Yao Li** – Center of Basic Molecular Science (CBMS), Department of Chemistry, Tsinghua University, Beijing 100084, China

Complete contact information is available at: <https://pubs.acs.org/doi/10.1021/acs.orglett.0c02128>

### Notes

The authors declare no competing financial interest.

## ■ ACKNOWLEDGMENTS

We thank the Natural Science Foundation of China (21861132003, 21672217, and 21521002) and Tsinghua University Initiative Scientific Research Program and The Netherlands Organization for Scientific Research (NWO-NSFC joint project) for financial support. S.L. is supported by the National Program of Top-notch Young Professionals. We thank the "BT mass spec facility of TU Delft" for the HRMS measurement.

## ■ REFERENCES

- (1) Kölmel, D. K.; Kool, E. T. Oximes and Hydrazones in Bioconjugation: Mechanism and Catalysis. *Chem. Rev.* **2017**, *117*, 10358–10376.
- (2) (a) Corbett, P. T.; Leclaire, J.; Vial, L.; West, K. R.; Wietor, J.-L.; Sanders, J. K. M.; Otto, S. Dynamic Combinatorial Chemistry. *Chem. Rev.* **2006**, *106*, 3652–3711. (b) Vantomme, G.; Jiang, S.; Lehn, J.-M. Adaptation in Constitutional Dynamic Libraries and Networks, Switching between Orthogonal Metalloselection and Photoselection Processes. *J. Am. Chem. Soc.* **2014**, *136*, 9509–9518. (c) Ulrich, S. Growing Prospects of Dynamic Covalent Chemistry in Delivery Applications. *Acc. Chem. Res.* **2019**, *52*, 510–519.
- (3) (a) Dirksen, A.; Hackeng, T. M.; Dawson, P. E. Nucleophilic Catalysis of Oxime Ligation. *Angew. Chem., Int. Ed.* **2006**, *45*, 7581–7584. (b) Dirksen, A.; Dirksen, S.; Hackeng, T. M.; Dawson, P. E. Nucleophilic Catalysis of Hydrazone Formation and Transimination: Implications for Dynamic Covalent Chemistry. *J. Am. Chem. Soc.* **2006**, *128*, 15602–15603. (c) Bhat, V. T.; Caniard, A. M.; Luksch, T.; Brenk, R.; Campopiano, D. J.; Greaney, M. F. Nucleophilic catalysis of acylhydrazone equilibration for protein-directed dynamic covalent chemistry. *Nat. Chem.* **2010**, *2*, 490–497.
- (4) (a) Mukherjee, S.; Bapat, A. P.; Hill, M. R.; Sumerlin, B. S. Oximes as reversible links in polymer chemistry: dynamic macromolecular stars. *Polym. Chem.* **2014**, *5*, 6923–6931. (b) Folmer-Andersen, J. F.; Lehn, J.-M. Thermoresponsive Dynamers: Thermally Induced, Reversible Chain Elongation of Amphiphilic Poly-(acylhydrazones). *J. Am. Chem. Soc.* **2011**, *133*, 10966–10973.
- (5) (a) Boekhoven, J.; Poolman, J. M.; Maity, C.; Li, F.; van der Mee, L.; Minkenberg, C. B.; Mendes, E.; van Esch, J. H.; Eelkema, R. Catalytic control over supramolecular gel formation. *Nat. Chem.* **2013**, *5*, 433–437. (b) Cai, M.; Han, Y.; Zhang, Q.; Luo, S. Aniline Catalysis in Bioconjugations and Material Synthesis. *Youji Huaxue* **2018**, *38* (1), 10. (c) Ryabchun, A.; Li, Q.; Lancia, F.; Aprahamian, I.; Katsonis, N. Shape-Persistent Actuators from Hydrazone Photoswitches. *J. Am. Chem. Soc.* **2019**, *141*, 1196–1200. (d) Ono, T.; Fujii, S.; Nobori, T.; Lehn, J.-M. Optodynamers: Expression of Color and Fluorescence at the Interface Between Two Films of Different Dynamic Polymers. *Chem. Commun.* **2007**, 4360–4362.
- (6) (a) Wolfenden, R.; Jencks, W. P. The Effect of *o*-Substituents on Benzaldehyde Semicarbazone Formation. *J. Am. Chem. Soc.* **1961**, *83*, 2763–2768. (b) Kool, E. T.; Park, D.-H.; Crisalli, P. Fast Hydrazone Reactants: Electronic and Acid/Base Effects Strongly Influence Rate at Biological pH. *J. Am. Chem. Soc.* **2013**, *135*, 17663–17666. (c) Kool, E. T.; Crisalli, P.; Chan, K. M. Fast Alpha Nucleophiles: Structures that Undergo Rapid Hydrazone/Oxime Formation at Neutral pH. *Org. Lett.* **2014**, *16*, 1454–1457. (d) Schmidt, P.; Zhou, L.; Tishinov, K.; Zimmermann, K.; Gillingham, D. Dialdehydes Lead to Exceptionally Fast Bioconjugations at Neutral pH by Virtue of a Cyclic Intermediate. *Angew. Chem., Int. Ed.* **2014**, *53*, 10928–10931. (e) Schmidt, P.; Stress, C.; Gillingham, D. Boronic acids facilitate rapid oxime condensations at neutral pH. *Chem. Sci.* **2015**, *6*, 3329–3333. (f) Wang, X.; Canary, J. W. Rapid Catalyst-Free Hydrazone Ligation: Protein-Pyridoxal Phosphoramides. *Bioconjugate Chem.* **2012**, *23*, 2329–2334. (g) Dilek, O.; Sorrentino, A. M.; Bane, S. Intramolecular Catalysis of Hydrazone Formation of Aryl-Aldehydes via ortho-Phosphate Proton Exchange. *Synlett* **2016**, *27*, 1335–1338. (h) Wang, S.; Gurav, D.; Oommen, O. P.; Varghese, O. P. Insights into the Mechanism and Catalysis of Oxime Coupling Chemistry at Physiological pH. *Chem. - Eur. J.* **2015**, *21*, 5980–5985. (i) Wang, S.; Nawale, G. N.; Kadekar, S.; Oommen, O. P.; Jena, N. K.; Chakraborty, S.; Hilborn, J.; Varghese, O. P. Saline Accelerates Oxime Reaction with Aldehyde and Keto Substrates at Physiological pH. *Sci. Rep.* **2018**, *8*, 2193.
- (7) (a) Cordes, E. H.; Jencks, W. P. Nucleophilic Catalysis of Semicarbazone Formation by Anilines. *J. Am. Chem. Soc.* **1962**, *84*, 826–831. (b) Cordes, E. H.; Jencks, W. P. On the Mechanism of Schiff Base Formation and Hydrolysis. *J. Am. Chem. Soc.* **1962**, *84*, 832–837. (c) Cordes, E. H.; Jencks, W. P. General Acid Catalysis of Semicarbazone Formation. *J. Am. Chem. Soc.* **1962**, *84*, 4319–4328. (d) Jencks, W. P. Studies on the Mechanism of Oxime and Semicarbazone Formation. *J. Am. Chem. Soc.* **1959**, *81*, 475–481.
- (8) (a) van der Helm, M. P.; Klemm, B.; Eelkema, R. Organocatalysis in aqueous media. *Nat. Rev. Chem.* **2019**, *3*, 491–508. (b) Rashidian, M.; Mahmoodi, M. M.; Shah, R.; Dozier, J. K.; Wagner, C. R.; Distefano, M. D. A Highly Efficient Catalyst for Oxime Ligation and Hydrazone–Oxime Exchange Suitable for Bioconjugation. *Bioconjugate Chem.* **2013**, *24*, 333–342. (c) Mahmoodi, M. M.; Rashidian, M.; Zhang, Y.; Distefano, M. D. Application of *meta*- and *para*-Phenylenediamine as Enhanced Oxime Ligation Catalysts for Protein Labeling, PEGylation, Immobilization, and Release. *Curr. Protoc. Protein Sci.* **2015**, *79*, 15.4.1–15.4.28. (d) Wendeler, M.; Grinberg, L.; Wang, X.; Dawson, P. E.; Baca, M. Enhanced Catalysis of Oxime-Based Bioconjugations by Substituted Anilines. *Bioconjugate Chem.* **2014**, *25*, 93–101. (e) Yuen, L. H.; Saxena, N. S.; Park, H. S.; Weinberg, K.; Kool, E. T. Dark Hydrazone Fluorescence Labeling Agents Enable Imaging of Cellular Aldehydic Load. *ACS Chem. Biol.* **2016**, *11*, 2312–2319.
- (9) (a) Crisalli, P.; Kool, E. T. Water-Soluble Organocatalysts for Hydrazone and Oxime Formation. *J. Org. Chem.* **2013**, *78*, 1184–1189. (b) Larsen, D.; Pittelkow, M.; Karmakar, S.; Kool, E. T. New Organocatalyst Scaffolds with High Activity in Promoting Hydrazone and Oxime Formation at Neutral pH. *Org. Lett.* **2015**, *17*, 274–277.
- (10) (a) Crisalli, P.; Kool, E. T. Importance of ortho Proton Donors in Catalysis of Hydrazone Formation. *Org. Lett.* **2013**, *15*, 1646–1649. (b) Larsen, D.; Kietrys, A. M.; Clark, S. A.; Park, H. S.; Ekebergh, A.; Kool, E. T. Exceptionally rapid oxime and hydrazine formation promoted by catalytic amine buffers with low toxicity. *Chem. Sci.* **2018**, *9*, 5252–5259.
- (11) (a) Drienovská, I.; Mayer, C.; Dulson, C.; Roelfes, G. A designer enzyme for hydrazone and oxime formation featuring an unnatural catalytic aniline residue. *Nat. Chem.* **2018**, *10*, 946–952. (b) Roelfes, G. LmrR: a privileged scaffold for artificial metalloenzymes. *Acc. Chem. Res.* **2019**, *52*, 545–556.
- (12) Erkkilä, A.; Majander, I.; Pihko, P. M. Iminium Catalysis. *Chem. Rev.* **2007**, *107*, 5416–5470.
- (13) Hemalatha, M. R. K.; Noorbach, I. An Undergraduate Physical Chemistry Experiment on the Analysis of First-Order Kinetic Data. *J. Chem. Educ.* **1997**, *74*, 972–974.
- (14) Yang, D.; Zuccarello, G.; Mattes, B. R. Physical Stabilization or Chemical Degradation of Concentrated Solutions of Polyaniline Emeraldine Base Containing Secondary Amine Additives. *Macromolecules* **2002**, *35*, 5304–5313.
- (15) Lv, J.; Zhang, Q.; Cai, M.; Han, Y.; Luo, S. Aromatic Aminocatalysis. *Chem. - Asian J.* **2018**, *13*, 740–753.
- (16) Vargas, E. L.; Velázquez, J. A.; Rodrigo, E.; Reinecke, H.; Rodríguez-Hernández, J.; Fernández-Mayoralas, A.; Gallardo, A.; Cid, M. B. pKa Modulation of Pyrrolidine-Based Catalytic Polymers Used for the Preparation of Glycosyl Hydrazides at Physiological pH and Temperature. *ACS Appl. Bio Mater.* **2020**, *3*, 1955–1967.
- (17) Aubry, C.; Wilson, A. J.; Emmerson, D.; Murphy, E.; Chan, Y. Y.; Dickens, M. P.; García, M. D.; Jenkins, P. R.; Mahale, S.; Chaudhuri, B. Fascaplysin-inspired diindolyls as selective inhibitors of CDK4/cyclin D1. *Bioorg. Med. Chem.* **2009**, *17*, 6073–6084.
- (18) Trausel, F.; Fan, B.; van Rossum, S. A. P.; van Esch, J. H.; Eelkema, R. Aniline Catalysed Hydrazone Formation Reactions Show

a Large Variation in Reaction Rates and Catalytic Effects. *Adv. Synth. Catal.* **2018**, *360*, 2571–2576.

(19) (a) Lovrak, M.; Hendriksen, W. E.; Kreutzer, M. T.; van Steijn, V.; Eelkema, R.; van Esch, J. H. Control over the Formation of Supramolecular Material Objects Using Reaction-Diffusion. *Soft Matter* **2019**, *15*, 4276–4283. (b) Maity, C.; Hendriksen, W. E.; van Esch, J. H.; Eelkema, R. Spatial Structuring of a Supramolecular Hydrogel using a Visible-light Triggered Catalyst. *Angew. Chem., Int. Ed.* **2015**, *54*, 998–1001. (c) Trausel, F.; Versluis, F.; Maity, C.; Poolman, J. M.; Lovrak, M.; van Esch, J. H.; Eelkema, R. Catalysis of Supramolecular Hydrogelation. *Acc. Chem. Res.* **2016**, *49*, 1440–1447.

(20) (a) Cagno, V.; Andreozzi, P.; D'Alicarnasso, M.; Jacob Silva, P.; Mueller, M.; Galloux, M.; Le Goffic, R.; Jones, S. T.; Vallino, M.; Hodek, J.; Weber, J.; Sen, S.; Janeček, E.-R.; Bekdemir, A.; Sanavio, B.; Martinelli, C.; Donalisio, M.; Rameix Welti, M.-A.; Eleouet, J.-F.; Han, Y.; Kaiser, L.; Vukovic, L.; Tapparel, C.; Král, P.; Krol, S.; Lembo, D.; Stellacci, F. Broad-spectrum non-toxic antiviral nanoparticles with a virucidal inhibition mechanism. *Nat. Mater.* **2018**, *17*, 195–203. (b) Jones, S. T.; Cagno, V.; Janeček, M.; Ortiz, D.; Gasilova, N.; Piret, J.; Gasbarri, M.; Constant, D. A.; Han, Y.; Vuković, L.; Král, P.; Kaiser, L.; Huang, S.; Constant, S.; Kirkegaard, K.; Boivin, G.; Stellacci, F.; Tapparel, C. Modified cyclodextrins as broad-spectrum antivirals. *Sci. Adv.* **2020**, *6*, eaax9318.

(21) (a) Poolman, J. M.; Maity, C.; Boekhoven, J.; van der Mee, L.; le Sage, V. A. A.; Groenewold, G. J. M.; van Kasteren, S. I.; Versluis, F.; van Esch, J. H.; Eelkema, R. A toolbox for controlling the properties and functionalisation of hydrazone-based supramolecular hydrogels. *J. Mater. Chem. B* **2016**, *4*, 852–858. (b) Wang, Y.; Xu, Z.; Lovrak, M.; le Sage, V. A. A.; Zhang, K.; Guo, X.; Eelkema, R.; Mendes, E.; van Esch, J. H. Biomimetic strain-stiffening self-assembled hydrogels. *Angew. Chem., Int. Ed.* **2020**, *59*, 4830–4834.